On pattern formation mechanism of $2+1$D max-plus models

Daisuke Takahashi‡, Atsuhiko Shida and Motohiro Usami

Department of Mathematical Sciences, Waseda University, 3-4-1, Ohkubo, Shinjuku-ku, Tokyo 169-8555, JAPAN

Abstract. We propose a max-plus equation which reproduce evolutional patterns often observed in reaction-diffusion systems of excitable media. The equation gives a travelling wave, a target pattern and a spiral pattern from appropriate initial data. Moreover, using advantages of max-plus equations, we obtain the solutions exactly by a reduction from the high-dimensional equation to a lower one. In the reduction, we use coordinate curves according to a shape of pattern. It is interesting that all patterns satisfy the same reduced equation. We also propose two other models similar to the previous one and discuss behavior of solutions.

PACS numbers: 45.70.Qj, 47.54.+r, 05.45.-a

‡ daisuke@mse.waseda.ac.jp

1. Introduction

Max-plus algebra is constructed from max operation as 'addition' and addition as 'multiplication' [1]. The followings show correspondence between usual real number operations and max-plus operations;

$$\begin{aligned}
a+b &\leftrightarrow \max(A,B),\\
ab &\leftrightarrow A+B,\\
a/b &\leftrightarrow A-B,\\
a+(b+c)=(a+b)+c &\leftrightarrow \max(A,\max(B,C))=\max(\max(A,B),C)\\
&\qquad\qquad =\max(A,B,C),\\
a(bc)=(ab)c &\leftrightarrow A+(B+C)=(A+B)+C,\\
a(b+c)=ab+ac &\leftrightarrow A+\max(B,C)=\max(A+B,A+C).
\end{aligned}$$

Since 'subtraction' $(a-b)$ is not defined in max-plus algebra without a special condition, we can not automatically transform an equation and its solutions including four arithmetic operations into those including max-plus operations. However, various 'integrable' max-plus equations were found by taking an ultradiscrete limit of integrable difference equations using formulae [2–5];

$$\begin{aligned}
&\lim_{\varepsilon\to+0}\varepsilon\log(e^{A/\varepsilon}+e^{B/\varepsilon}+\cdots)=\max(A,B,\cdots),\\
&(\lim_{\varepsilon\to+0})\varepsilon\log(e^{A/\varepsilon}e^{B/\varepsilon}\cdots)=A+B+\cdots.
\end{aligned}\tag{1}$$

Difference special solutions like N-soliton solutions can also be transformed into max-plus ones. Though max-plus solutions can be derived from corresponding difference ones, we can confirm that they satisfy the equation by a direct substitution using max-plus operations.

Another feature of max-plus equation is a discreteness of dependent variable. Let us consider the ultradiscrete Burgers equation [6]

$$U_j^{t+1}=U_{j-1}^t+\max(1,U_j^t+U_{j+1}^t)-\max(1,U_{j-1}^t+U_j^t),$$

as an example. (It can be 'linearized' by ultradiscrete Cole-Hopf transformation $U_j^t=F_{j+1}^t-F_j^t+1/2$ and we obtain $F_j^{t+1}=\max(F_{j-1}^t,F_{j+1}^t)$.) We can consider the dependent variable U is continuous, but if initial values are all integer, U's are always integer. In this meaning, max-plus algebra can propose equations with all discrete variables. Moreover, we can easily show any U is always 0 or 1 if initial U's are so. It means the above equation can become a cellular automaton (CA) [7].

Considering the above features of max-plus equations, we meet a question "How many mechanisms in continuous mathematics survive in max-plus algebra?" Note that integrability is not necessary for max-plus operations. In this paper, we make max-plus models of a pattern formation mechanism, which give evolutional patterns often observed in reaction-diffusion systems of excitable media.

Reaction-diffusion systems show us a rich structure of pattern dynamics [8]. For example, in the Belouzov–Zhabotinsky (BZ) chemical reaction, two-dimensional ring-shaped reaction waves are repeatedly produced from a core area and they propagate

outward as concentric circles [9]. This pattern is called a 'target' pattern. Moreover, a single or a double 'spiral' pattern often appears. It turns around a core and its outer part propagates outward. The target and the spiral patterns are commonly observed in various reaction-diffusion systems. The systems are often modelled using two kinds of materials, activator and inhibitor, in a form of a couple of differential equations. Numerical simulations of the model equations can reproduce the pattern dynamics well.

Moreover, various CA models have been made to simulate the dynamics [10–17]. They are discrete analogues to pattern formation systems and their results match the phenomena well. Due to discreteness of CA models, we can obtain exact solutions even by numerical simulations. Local behavior of solutions can be easily checked by analyzing an evolution rule of the models. These are advantages of CA models. However, it is often difficult to discuss global or asymptotic properties of solutions in the CA models. On the other hand, we have accumulated many techniques to evaluate such properties for differential models. Our main purpose of this paper is to propose max-plus models including both advantages of CA and differential models. In the max-plus models, we can give exact solutions like those to CA models and can also show global behavior of the solutions using similar techniques to those of differential models.

In section 2, we propose a $2+1$D max-plus model and show that it has various solutions including target and spiral patterns. In section 3, we show that basic solutions to the model can be derived from a lower-dimensional equation obtained by a reduction using some coordinate curves. Travelling wave, target pattern and spiral pattern are all derived from solutions to the same 1D equation reduced by corresponding curves. In section 4, we show two other models obtained by a small modification of the original one. Though shape and behavior of the above basic solutions are slightly changed, they also exist stably in the models. In section 5, we give concluding discussions.

2. $2+1$D max-plus model

In this paper, we consider the following $2+1$D max-plus equation,

$$U_{ij}^{t+1} = \max(U_{i-1j}^{t}, U_{i+1j}^{t}, U_{ij-1}^{t}, U_{ij+1}^{t}, U_{ij}^{t}) - U_{ij}^{t} - U_{ij}^{t-1}, \tag{2}$$

where i and j are both spatial lattices and t is discrete time. We assume spatial lattices are infinite ($-\infty < i < \infty$ and $-\infty < j < \infty$) and $U_{ij}^{t} \to 0$ for $|i|, |j| \to \infty$. Then we can follow a time evolution of U if we set initial data at two successive time steps. Moreover, since (2) is symmetric on t, (2) is reversible in time.

Below we assume without loss of generality that $t = 0$ is an initial time for initial value problem of (2). If U_{ij}^{0} and U_{ij}^{1} are all integer, then U_{ij}^{t} is always integer. In this sense, we can consider a dependent variable U as well as independent variables i, j and t are all discrete. Moreover, if U is a solution to (2), cU is also where c is a constant. Using this property and considering piecewise linearity of (2), we easily see that an initial value problem using integer values is equivalent to that using rational ones. Therefore, we can discuss behavior of a wide range of solutions by investigating only integer solutions.

Figure 1 shows an example of basic solution to (2). Values 1, 2 and 3 make vertical lines respectively with enough 0's between them and initial data satisfy $U^1_{ij} = U^0_{i-1j}$. Then, a solution obtained always satisfies $U^{t+1}_{ij} = U^t_{i-1j}$. Thus the non-zero lines become travelling waves with speed $(1, 0)$, not interacting each other. If we set initial data at $t = 1$ by $U^1_{ij} = U^0_{i+1j}$, then travelling waves with speed $(-1, 0)$ are obtained. Generally, there are waves travelling in directions $(\pm 1, 0)$ or $(0, \pm 1)$ from appropriate initial data.

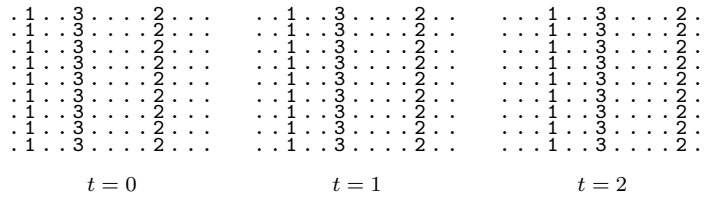

Figure 1. Travelling waves. Character '.' denotes 0.

Figure 2 shows a 'single ring' pattern. U^0_{ij} and U^1_{ij} are all 0 except that U^1_{ij} at a certain lattice point is 1. From that point, a diamond-shaped wave with value 1 spreads outward.

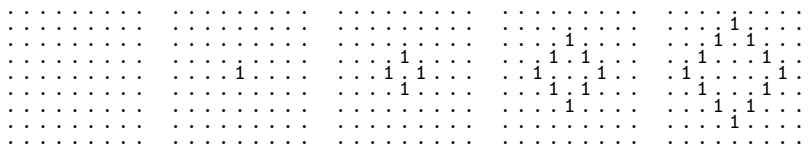

Figure 2. Single ring pattern.

Figure 3 shows a process to form a stable 'target' pattern. At the center point, the value changes periodically as 1, 1, -1 and diamond-shaped waves appear and spread outward repeatedly with period 3.

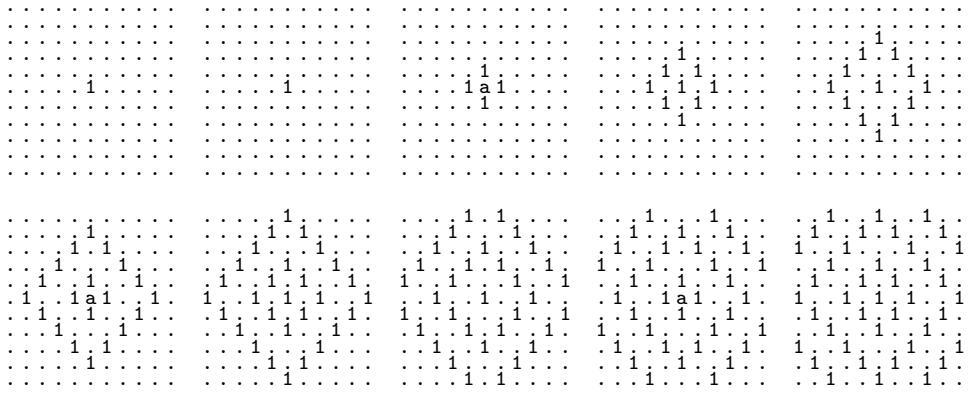

Figure 3. Target pattern. Character 'a' denotes -1.

Figure 4 shows a process to form a stable 'spiral' pattern. From an infinite line of value 1, we obtain a simple travelling wave like those in Fig. 1. If we use a half-line

instead, a spiral appears from its end point. After an infinite time, the spiral spreads through the whole space region and it rotates by 90 degrees per unit time.

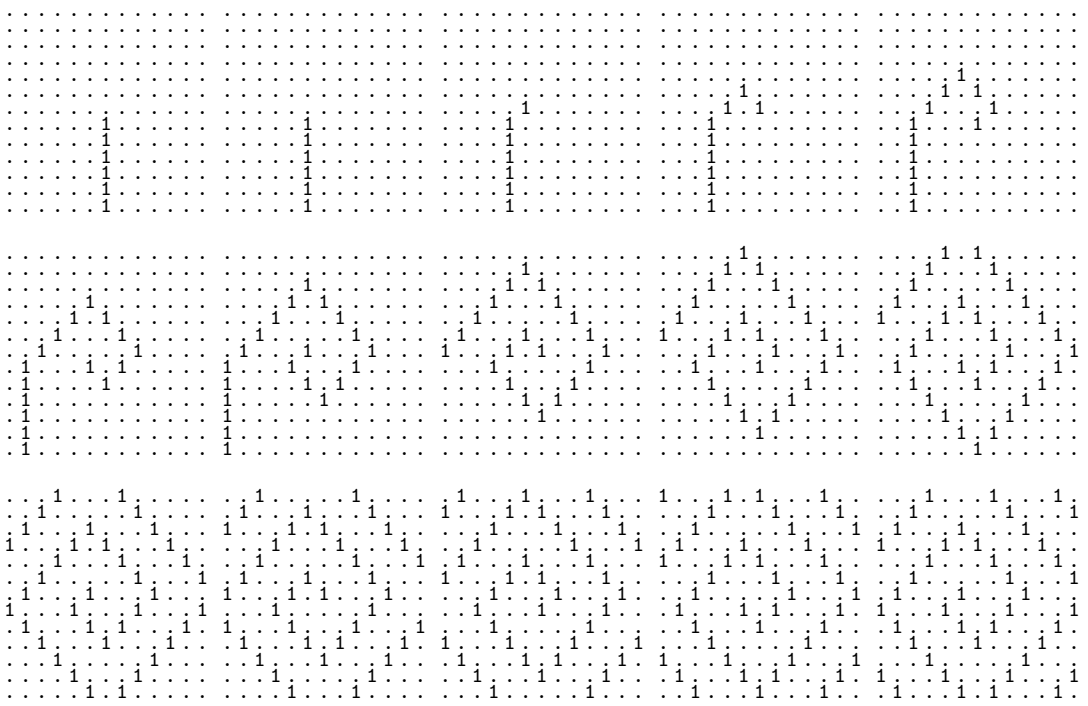

Figure 4. Spiral pattern.

We can consider the above target and spiral patterns are discrete analogues to those commonly observed in various reaction-diffusion systems. In the systems, activator and inhibitor play important roles to make patterns. For example, Belouzov–Zhabotinsky reaction system is often modelled in a form of

$$\begin{cases} u_t = D_u \Delta u + f(u,v) \\ v_t = D_v \Delta v + g(u,v) \end{cases}, \tag{3}$$

where D_u and D_v are diffusion coefficients and f and g are reaction terms [8]. State variables $u(x,y,t)$ and $v(x,y,t)$ are 'activator' and 'inhibitor' respectively. Equation (3) is a system of first order differential equations on time. $D_u\Delta u$ and $D_v\Delta v$ have two dimensional diffusion effect and f and g have reaction effect between u and v. On the other hand, (2) is a single difference equation of second order on time. We can rewrite (2) to the following couple of equations using an auxiliary variable $V_{ij}^t = U_{ij}^{t-1}$;

$$\begin{cases} U_{ij}^{t+1} = \max(U_{i-1j}^t, U_{i+1j}^t, U_{ij-1}^t, U_{ij+1}^t, U_{ij}^t) - U_{ij}^t - V_{ij}^t \\ V_{ij}^{t+1} = U_{ij}^t \end{cases}. \tag{4}$$

Both equations are of first order on time. Since the max term in the first equation includes von Neumann neighborhoods of U_{ij}^t, information on a lattice point propagates to surrounding ones. Let us consider the following equation

$$U_{ij}^{t+1} = \max(U_{i-1j}^t, U_{i+1j}^t, U_{ij-1}^t, U_{ij+1}^t, U_{ij}^t) - U_{ij}^t, \tag{5}$$

which is made from the first equation of (4) by removing the last term in its right-hand side. If we set $U_{ij}^0 = 0$ other than $U_{00}^0 = 1$, then we obtain a time evolution as shown in Fig. 5. We easily see from (5) that $U_{ij}^{t+1} \geq 0$ generally and a localized positive value of U spreads outward. In this rough meaning, U can be regarded as activator.

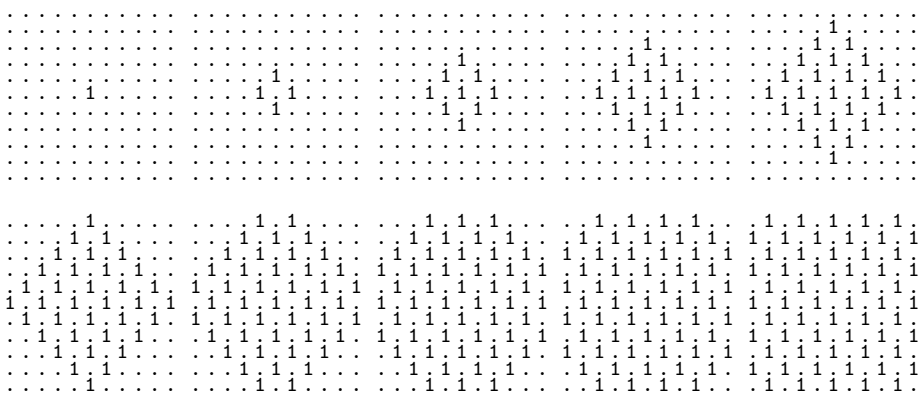

Figure 5. Time evolution of a solution to (5).

Existence of V in the first equation of (4) means that U at the next time decreases if a current V is positive. Moreover, though current V is 0, V grows if current U is positive, according to the second equation. It means V plays a role of inhibitor.

From the above discussion, we can consider (4) is a rough sketch of reaction-diffusion system. However, the above arguments are only the bare minimum of reaction-diffusion system. They do not fully account for occurrence of target and spiral patterns. In the next section, we make further discussion about a reason why both patterns appear in (2).

3. Stable pattern and coordinate curves

When we derive a special solution to a high-dimensional differential equation, we often assume a symmetry of solution and obtain a lower-dimensional differential equation. For example, if we have a 2+1D PDE on $u(x, y, t)$ and assume an axisymmetric solution, we usually assume $u = v(r, t)$ with polar coordinate (r, θ) and reduce the 2+1D PDE to 1+1D. Moreover, if we would get a travelling wave solution for $v(r, t)$, we assume $v(r, t) = w(z)$ where $z = r - ct$ and obtain an ODE on z from the 1+1D PDE. We can show below that a similar procedure can be applied to (2) and all patterns in Figs. 1–4 satisfy the same ordinary difference equation.

Let us consider a family of lines defined by $i = \text{const}$ and label each line by its i-coordinate. Moreover, if we assume that values of U_{ij}^0 on the n-th line are the same and those of U_{ij}^1 are also, values of U_{ij}^t on the n-th line are always the same according to (2). Then, if F_n^t denotes the same value of U_{ij}^t on the n-th line at time t, F_n^t satisfies the following equation;

$$F_n^{t+1} = \max(F_{n-1}^t, F_n^t, F_{n+1}^t) - F_n^t - F_n^{t-1}, \tag{6}$$

because $\max(U^t_{i-1j}, U^t_{i+1j}, U^t_{ij-1}, U^t_{ij+1}, U^t_{ij})$ reduces to $\max(F^t_{n-1}, F^t_n, F^t_{n+1})$.

Moreover, if we consider a travelling wave solution $F^t_n = G_{n\pm t}$ with speed ∓ 1, G_n satisfies

$$G_{n-1} + G_n + G_{n+1} = \max(G_{n-1}, G_n, G_{n+1}), \tag{7}$$

by a reduction of (6). This equation does not determine a solution uniquely from initial data. To obtain a general solution to (7), let us consider the following equation on A, B and C,

$$A + B + C = \max(A, B, C), \tag{8}$$

where $A \le B \le C$. Since a value of right-hand side is equal to C, $A + B = 0$ is derived. Therefore, we obtain $(A, B, C) = (-\alpha, \alpha, \beta)$ where $0 \le \alpha \le \beta$. Thus, if G_{n-1}, G_n and G_{n+1} satisfy a local condition

$$\{G_{n-1}, G_n, G_{n+1}\} = \{-\alpha, \alpha, \beta\}, \tag{9}$$

for any n, G becomes a solution to (7). Since a boundary condition on U is $\lim_{|i|,|j|\to\infty} U^t_{ij} = 0$, that for G is $\lim_{|n|\to\infty} G_n = 0$. Therefore, a general solution to (7) considering the boundary condition has a pattern of values as follows;

$$\cdots 000 p_1 0 * 0 p_2 0 * 0 p_3 0 * \cdots\cdots * 0 p_m 000 \cdots,$$

where p_1, p_2, $\cdots$, p_m are all positive numbers and $*$ means nothing or some 0's. As for the solution in Fig. 1, $G = \cdots 000100300002000 \cdots$.

Other travelling wave solutions to (2) can be obtained by other symmetries of a solution. Consider a family of polygonal curves of infinite length reaching $j \to \pm\infty$ as shown in Fig. 6. All curves have the same shape and all vertices are on lattice points. Moreover, all segments on a curve is any of $(i, j) - (i - 1, j + 1)$, $(i, j) - (i, j + 1)$ or $(i, j) - (i - 1, j + 1)$.

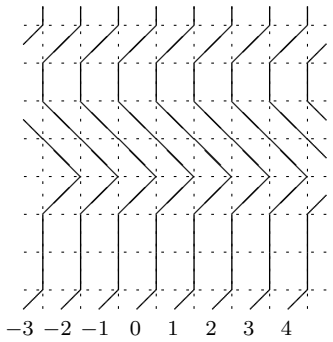

Figure 6. Example of a family of polygonal curves. Integers denote labels of the curves.

Let us label the curves sequentially with integers as shown in the figure. If we assume that all values of U^t_{ij} on each curve are the same, F^t_n denoting the value of U on a curve n at time t satisfies (6) because $\max(U^t_{i-1j}, U^t_{i+1j}, U^t_{ij-1}, U^t_{ij+1}, U^t_{ij})$ again reduces

to $\max(F^t_{n-1}, F^t_n, F^t_{n+1})$. Moreover, we can obtain a travelling wave solution $F^t_n = G_{n\pm t}$ satisfying (7). Note that there are travelling wave solutions obtained by rotating the solutions shown above by 90 degrees.

Surprisingly, single ring (Fig. 2), target (Fig. 3) and spiral (Fig. 4) patterns obey the same scenario as above. First, let us consider a family of diamond-shaped curves as shown in Fig. 7. and give a sequential integer as a label to each diamond. The center point is a special diamond with zero area.

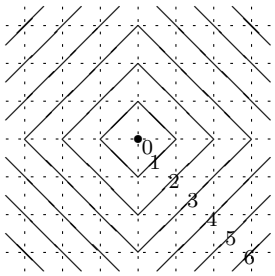

Figure 7. Family of diamond-shaped curves.

Consider an arbitrary lattice point (i, j) on n-th $(n > 0)$ diamond. Then, lattice points $(i \pm 1, j)$ and $(i, j \pm 1)$ are all on $(n-1)$-th or $(n+1)$-th diamond and both diamonds include at least one point among the points. Therefore, if we assume that values of U^t_{ij} on each diamond are the same, F^t_n denoting the value of U on the n-th diamond at time t satisfies (6) for $n > 0$. As for the center point, a boundary condition

$$F^{t+1}_0 = \max(F^t_0, F^t_1) - F^t_0 - F^{t-1}_0 \tag{10}$$

is applied. Under this condition, evolution pattern of F^t_n for a single ring and a target pattern are shown in Fig. 8 (a) and (b) respectively. Only one wave is produced from

$n=$	0	1	2	3	4
$t=0$	0	0	0	0	0
1	1	0	0	0	0
2	0	1	0	0	0
3	0	0	1	0	0
4	0	0	0	1	0

(a)

$n=$	0	1	2	3	4	5	6	7	8	9
$t=0$	1	0	0	0	0	0	0	0	0	0
1	1	0	0	0	0	0	0	0	0	0
2	−1	1	0	0	0	0	0	0	0	0
3	1	0	1	0	0	0	0	0	0	0
4	1	0	0	1	0	0	0	0	0	0
5	−1	1	0	0	1	0	0	0	0	0
6	1	0	1	0	0	1	0	0	0	0
7	1	0	0	1	0	0	1	0	0	0
8	−1	1	0	0	1	0	0	1	0	0

(b)

Figure 8. Evolution of F^t_n. (a) Single ring, (b) Target pattern.

the point $n = 0$ in the case of (a) and an infinite number of waves are periodically produced in the case of (b). Since a relation $F_n^{t+1} = F_{n-1}^t$ is satisfied for $n \geq 1$ in (a) and for $n \geq 2$ in (b), we can consider travelling waves are produced from a boundary condition on the point $n = 0$.

Secondly, let us consider a family of four spiral curves as shown in Fig. 9. They have

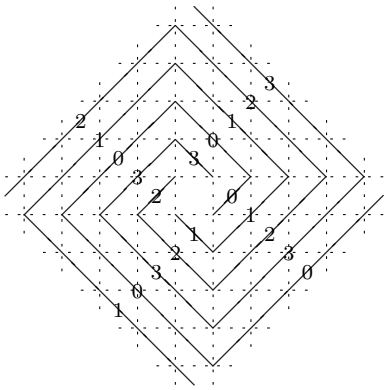

Figure 9. Four spiral curves.

the same shape and cover all lattice points in the plane. Nearest neighboring points of any point on a curve n are on a curve $n-1$ or $n+1$ modulo 4. Therefore, if we assume all U's on each curve are the same, (2) reduces to (6) through F_n^t denoting a value of U on a curve n at time t. The variable n of F_n^t is periodic with period 4 or finite with modulus 4. Again we can consider a travelling wave solution $F_n^t = G_{n\pm t}$ and it satisfies (7). Since there is a restriction (9) for G_n, we obtain $\{G_0, G_1, G_2, G_3\} = \{0, 0, 0, \alpha\}$ where $\alpha > 0$. We can easily see that a completely developed spiral pattern obtained at $t \to \infty$ in Fig. 4 satisfies (7) using the four spiral curves and the reduction above. Note that we can not explain the whole evolution of solution shown in Fig. 4 because initial data do not satisfy the equality condition of values on four spiral curves. We add a notice that there is a reversely-winding spiral obtained from a mirror image of the above spiral curves.

There are many other evolutional patterns satisfying (7) with other families of curves and the same reduction. Figure 10 shows such examples. If we assume all values are the same on each curve for initial data, we can obtain a double target pattern from Fig. 10 (a) and a double spiral one from (b). We can easily see that some targets and/or spirals can coexist like these examples and it is true for various reaction-diffusion systems. However, if we set two cores of targets with value 1 and with value 2 apart from each other, their interaction is complicated and the target pattern with value 2 often destroys that with 1 after enough time.

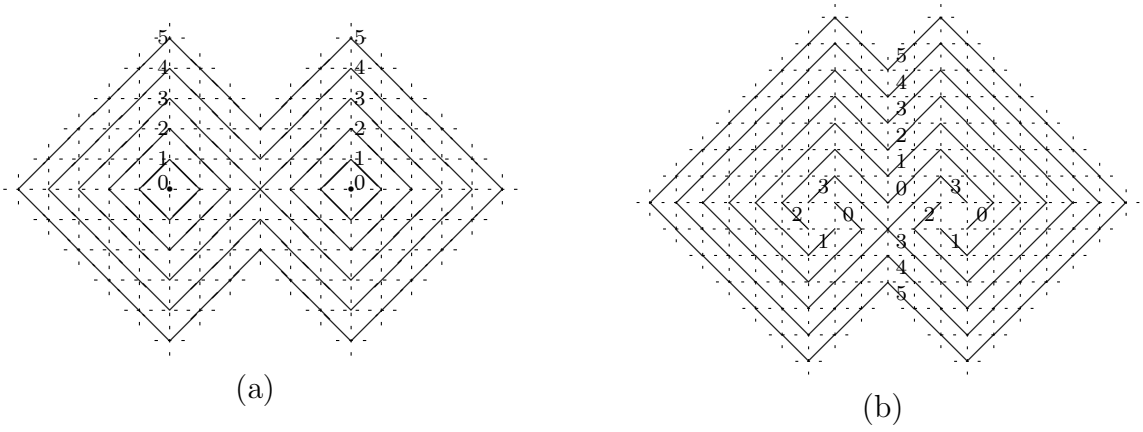

Figure 10. Curves for (a) a double target, (b) a double spiral.

4. Other models

In the previous section, we have shown a symmetry of (2) makes stable patterns tracing coordinate curves. However, this symmetry is not peculiar to (2) and there are other max-plus models showing the patterns. For example, a model equation

$$U_{ij}^{t+1} = \max(U_{i-1j}^t, U_{i+1j}^t, U_{ij-1}^t, U_{ij+1}^t, U_{ij}^t) - U_{ij}^{t-1}, \tag{11}$$

gives also travelling wave, target pattern, spiral pattern and their multiple pattern. A difference from (2) is a lack of term $-U_{ij}^t$ in the right-hand side. This equation can be reduced to

$$F_n^{t+1} = \max(F_{n-1}^t, F_n^t, F_{n+1}^t) - F_n^{t-1}, \tag{12}$$

using the same assumption in the previous section. Since a travelling wave solution satisfies

$$G_{n-1} + G_{n+1} = \max(G_{n-1}, G_n, G_{n+1}), \tag{13}$$

its local value pattern is $0\,b\,a$ or $a\,b\,0$ where $a \geq 0$ and $a \geq b$, or $a\,a+b\,b$ where $a \geq 0$ and $b \geq 0$. It means that a local pattern $0\,c\,0$ ($c \geq 0$) can not be allowed and $0\,c\,c\,0$ is possible. Therefore a width of localized waves becomes wider. Figure 11 shows a periodic double spiral pattern with period 4. Note that coordinate curves are of the same type of those in Fig. 10 (b) and a width of spiral becomes wider than that in Fig. 4.

Another example of model is the following,

$$U_{ij}^{t+1} = \max(U_{i-1j}^t, U_{i+1j}^t, U_{ij-1}^t, U_{ij+1}^t, U_{ij}^t, U_{ij}^{t-1}) - U_{ij}^{t-1}. \tag{14}$$

An additional term U_{ij}^{t-1} is introduced into the max term of (11). Using coordinate curves, this equation reduces to

$$F_n^{t+1} = \max(F_{n-1}^t, F_n^t, F_{n+1}^t, F_n^{t-1}) - F_n^{t-1},$$

and travelling wave solutions satisfy the same equation as (13). Since the max term of (14) includes U_{ij}^{t-1}, we derive $U_{ij}^{t+1} \geq 0$. Moreover, we easily see that U_{ij}'s at time $t+1$

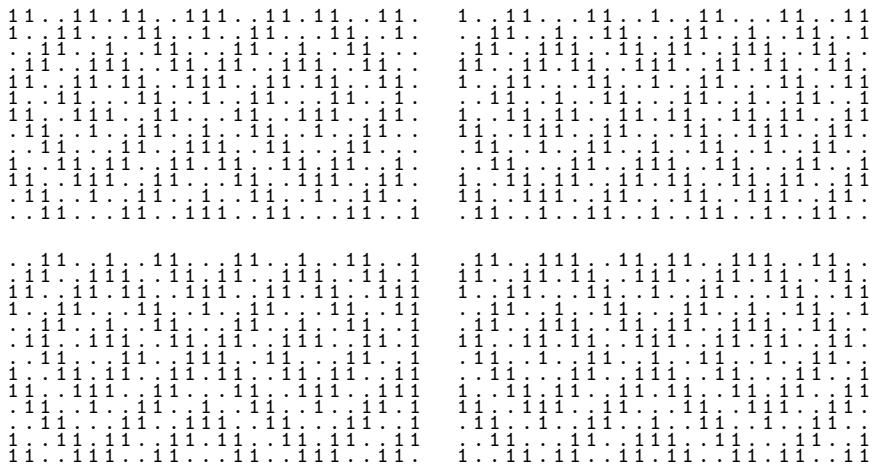

Figure 11. Double spiral pattern given by (11). It is also a solution to (14).

can not exceed the maximum value among those at time t. Therefore, if $0 \leq U_{ij}^0 \leq L$ and $0 \leq U_{ij}^1 \leq L$ where L is a positive integer, U_{ij}^t is also. Especially, if U_{ij}^0 and U_{ij}^1 are all 0 or L, U_{ij}^t is also. In this meaning, (14) constructs a CA depending on initial data. Since the solution to (11) shown in Fig. 11 includes only 0 and 1, it also becomes a solution to (14).

Moreover, if all U_{ij}^t are always 0 or L (> 0) as described above, we can show existence of 'tough' cores of target and spiral patterns. In this case, if $U_{ij}^{t-1} = 0$ and $U_{ij}^t = L$, then $U_{ij}^{t+1} = L$, $U_{ij}^{t+2} = 0$ and $U_{ij}^{t+3} = 0$ are obtained from (14). Moreover, if $U_{ij}^{t-1} = U_{ij}^t = 0$ and at least one of $U_{i\pm1j}^t$ and $U_{ij\pm1}^t$ is L, then $U_{ij}^{t+1} = L$ is derived. Therefore, an evolution of a local pattern shown in Fig. 12 is stable and periodic with period 4. This becomes a core of target pattern because the value L appears repeatedly at the center point and its copies propagate neighboring sites. Another tough core is shown in Fig. 13 and it is also periodic with period 4. This is a core of spiral pattern and we can observe the same cores in Fig. 11.

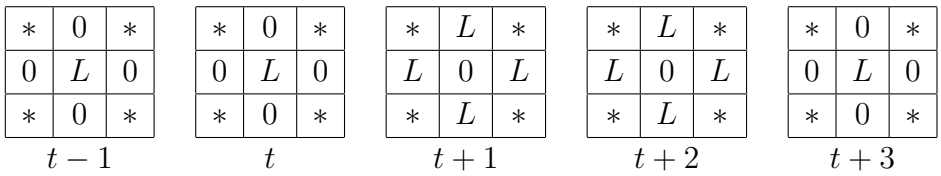

Figure 12. Core of target pattern of (14). $*$ denotes 0 or L.

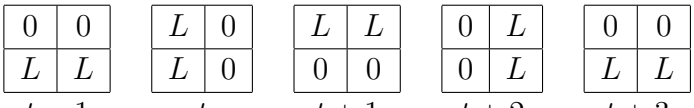

Figure 13. Core of spiral pattern of (14).

5. Concluding discussions

In this paper, we presented a max-plus model (2) showing a pattern formation mechanism. It gives travelling waves, target patterns and spiral patterns. Target and spiral patterns are stable and multiple target or spiral patterns also. The remarkable feature of the model is that we can show such patterns by exact solutions using the reduction of high-dimensional equation to lower dimension with coordinate curves, as we often do for high-dimensional differential equations.

We also showed two other models (11) and (14) by removing or adding a few terms. Despite the modification, target and spiral patterns survive and their solutions are derived by the similar reduction process. In the latter model, we showed it can construct a CA under a restriction and an evolution of core is not effected by surrounding sites. It is interesting that the similar type of equations give the similar dynamics. This is generally true for the real reaction-diffusion systems and their mathematical models.

Next, we give interesting future problems related to the above models. The first problem is analyzing a general dynamics from arbitrary initial data. We showed only specific patterns from selected initial data made from two integer values. Our numerical simulations from more general data suggest a complicated evolutional dynamics, sometimes a chaotic behavior. Note that our models give a stable basic pattern of an arbitrary value. If U_{ij}^t is a solution, then $c\,U_{ij}^t$ is also. On the other hand, a value of uniform solution to known differential models changes between two stable values periodically, and bottom and top area of a localized wave take either of the values. We consider this different property of our models from the differential models reflects complex dynamics of our models. In this meaning, physical interpretation of our models should be discussed.

Our models can propose a clear analysis on various characteristic patterns. Exact solutions of the whole region including core area is rarely obtained for differential systems. Our models are fully discrete and it makes analysis easier. Though considering this advantage, reduction of the equation with coordinate curves is a parallel procedure to those done for differential systems. Note that known CA models showing the patterns are usually described by Boolean operation or procedural words and such an analysis is rarely successful. We hope a strong link between our models and differential systems utilizing above features of our models, like integrable max-plus equations.

We give two remarks below in order to suggest this link. First, consider a finite difference equation

$$g_{n-1}g_ng_{n+1} = g_{n-1} + g_n + g_{n+1}. \tag{15}$$

If we use a transformation $g_n = e^{G_n/\varepsilon}$ and take a limit $\varepsilon \to +0$, we get (7) using formulae (1). Moreover (15) reduces to $\theta_{n-1} + \theta_n + \theta_{n+1} = k_n\pi$ where $g_n = \tan\theta_n$ and k_n is an arbitrary integer depending on n. One of solutions to this equation is $\theta_n : \cdots \frac{\pi}{4}, \frac{\pi}{4}+\delta, \frac{\pi}{2}-\delta, \frac{\pi}{4}, \frac{\pi}{4}+\delta, \frac{\pi}{2}-\delta, \cdots$. If we use $\delta = e^{-1/\varepsilon}$ and take a limit $\varepsilon \to +0$, we obtain $G_n : \cdots 0\,0\,1\,0\,0\,1 \cdots$. This is a solution to (7). Though we can not give a

general solution of G_n from (15), we can consider (15) is a suggestive example to show a relationship between continuous and discrete models.

Secondly, consider the following difference equation;

$$u_{ij}^{t+1} + u_{ij}^{t} + u_{ij}^{t-1} \quad = \log[\alpha(e^{u_{i+1j}^{t}} + e^{u_{i-1j}^{t}} + e^{u_{ij+1}^{t}} + e^{u_{ij-1}^{t}}) + \beta e^{u_{ij}^{t}}], \quad (16)$$

where α and β are positive constants. If we use a transformation $u_{ij}^{t} = U_{ij}^{t}/\varepsilon$ and take an ultradiscrete limit $\varepsilon \to +0$, we obtain (2) directly. Moreover, if we assume $u_{ij}^{t} = v(hi, hj, ht)$ and $h \sim 0$, we obtain

$$v_{tt} \sim \frac{\alpha}{4\alpha+\beta}(\Delta v + |\nabla v|^2) + \frac{1}{h^2}(\log(4\alpha+\beta) - 2v). \quad (17)$$

When we use initial data of u_{ij}^{t} corresponding to U_{ij}^{t} with finite ε and calculate a time evolution of (16) numerically, we can observe patterns described in the previous sections if ε is small enough. However, the patterns do not survive eternally and they disappear after a long time. When ε is not small ($\varepsilon \sim 1$), the patterns disappear more quickly. Moreover, we can not observe the patterns surviving for a long time in the numerical calculations of (17) .

(16) is not a unique equation reducing to (2) and we can make many other examples. Therefore, it is an important future problem to find a difference and a differential equations which are directly related to (2) through ultradiscretization and give a similar patern mechanism.

References

[1] Baccelli F, Cohen G, Olsder G J and Quadrat J P 1992 *Synchronization and Linearization* (John Wiley & Son)
[2] Tokihiro T, Takahashi D, Matsukidaira J and Satsuma J 1996 *Phys. Rev. Lett.* **76** 3247
[3] Hirota R, Iwao M, Ramani A, Takahashi D, Grammaticos B and Ohta Y 1997 *Phys. Lett.* A **236** 39
[4] Ramani A, Takahashi D, Grammaticos B and Ohta Y 1998 *Physica* D **114** 185
[5] Tokihiro T, Takahashi D and Matsukidaira J 2000 *J. Phys.* A **33** 607
[6] Nishinari K and Takahashi D 1998 *J. Phys.* A **31** 5439
[7] Wolfram S 1986 *Theory and Applications of Cellular Automata* (Singapore: World Scientific)
[8] Meron E 1992 *Phys. Rep.* **218** 1
[9] Winfree A T 1974 *Sci. Am.* **230** 82
[10] Moe G K, Rheinboldt W C and Abildskov J A 1964 *Am. Heart J.* **67** 200
[11] Greenberg J M and Hastings S P 1978 *Siam J. Appl. Math.* **34** 515
[12] Greenberg J M, Hassard B D and Hastings S P 1978 *Bull. Am. Math. Soc.* **84** 1296
[13] Greenberg J M, Greene C and Hastings S P 1978 *Siam J. Alg. Disc. meth.* **1** 34
[14] Hartman H and Tamayo P 1990 *Physica* D **45** 293
[15] Gerhardt M and Schuster H 1989 *Physica* D **36** 209
[16] Gerhardt M, Schuster H and Tyson J J 1990 *Physica* D **46** 392
[17] Gerhardt M, Schuster H and Tyson J J 1990 *Physica* D **46** 416